Effect of a Novel Polysilicone on the Flame Retardancy and Thermal Degradation of Epoxy Resin

JIANGBO WANG*

School of Materials and Chemical Engineering, Ningbo University of Technology, Ningbo 315211, China

ABSTRACT

In the present study, a novel polysilicone PMDA was synthesized and the effect of PMDA on the flame retardancy of epoxy resin (EP) was investigated by cone calorimeter measurement. EP/PMDA (FREP) composite exhibited lower peak heat release rate (PHRR) and total heat release (THR) in comparison with those of pure EP, indicating the higher fire safety of FREP. Furthermore, the thermal degradation behavior of FREP composite was investigated by the TGA measurement under non-isothermal conditions. The Kissinger and Flynn-Wall-Ozawa methods were both used to analyze the thermal degradation process of EP composites. The results illustrated that PMDA remarkable enhanced the activation energies of EP thermal degradation in the final stage, revealing that the flame retardant PMDA stabilized the residual char layer and improved the flame retardancy of EP in the final period of thermal degradation process.

KEYWORDS: *Flame retardancy, Epoxy resin, Polysilicone, Thermal degradation, Flynn-Wall-Ozawa method*

1. INTRODUCTION

Epoxy resins (EP) are a class of materials that are widely used in various industrial fields such as coating, potting, adhesives, laminates, and composites due to their excellent moisture, solvent and chemical resistance, toughness, high adhesion to many substrates, superior electrical and mechanical properties [1-4]. However, one of the main drawbacks of epoxy resin is its inherent flammability, which restricts its application in many fields for safety consideration [5-7]. Therefore, it is an important issue to improve the flame retardancy of epoxy resins. Although halogenated flame retardants show good flame retardancy and have been used widely for several decades, their use has

J. Polym. Mater. Vol. **35,** No. 1, 2018, 33-44

Correspondence author e-mail: jiangbowang@163.com

been curtailed in many countries because of the release of highly toxic and corrosive fumes during combustion and the bioaccumulated toxic substances produced [8-10]. For this reason, developing of halogen-free flame retardants has been one of the hot research fields recently.

In recent years, the development of silicon-containing flame retardants has acquired increasing importance, owing to their excellent thermal stability, flame retardancy moisture resistance, and low surface energy. While heating, low surface energy of silicon renders it to migrate to the surface of epoxy resins and to form a protective layer with high heat-resistance to avoid polymer residue from thermal degradation. Silicon is therefore considered as one of the 'environment friendly' fame-retarding elements. The conventional practice of introducing silicon-containing compounds into polymers has been achieved by blending those polymers with polydimethylsiloxanes. Most epoxy resins, such as the diglycidyl ether of bisphenol A (DGEBA), are carbon based, whereas the silicon-containing compounds are inorganic based; therefore they are usually immiscible and phase separation limits incorporation of a large amount of silicon compound [11-13]. Such limitation leads to a more serious problem of bleeding of silicon components. Therefore, in order to reduce the above limitation, polysilicones with reactive groups are utilized to prepare polymers that possess siloxane bond in the backbones or on side chains through grafting reactions [14-16].

Our previous work has described the synthesis of a branched polymethylphenylsiloxane (PMPSQ) used for flame retardant epoxy systems. The incorporation of PMPSQ into epoxy resin can improve its flame retardancy and char yield during combustion [11]. In this work, a novel amino-containing polysilicone (PMDA) has been prepared and evaluated as halogen-free flame retardants for epoxy resins. Effects of the PMDA on the flame retardancy and thermal stability of epoxy resins were investigated.

2. EXPERIMENTAL

2.1 Materials

Tetramethylammonium hydroxide (TMAOH), methyltrimethoxysilane (MTMS) and (3-aminopropyl) trimethoxysilane (APS) were all purchased from Alfa Aesar Chemical Reagent Co. Ltd. Phenyl trimethoxysilane (PTMS) and dimethyldimethoxysilane (DMDS) were reagent grade and purchased from Gelest Chemical Reagent Co. Ltd. Ethyl alcohol (EtOH) was supplied by Sigma-Aldrich. EPON 826 with an epoxy equivalent weight of 178-186 grams was supplied by Hexion and used as received. The hardener, Jeffamine D230, with an amine equivalent weight of 60 grams, was supplied by Huntsman Corporation and also used as received.

2.2 Synthesis of polysilicone (PMDA)

The polysilicone PMDA was synthesized by hydrolysis and condensation, consisted of 60 mol% phenylsiloxane, 35 mol% methylsiloxane and 5 mol% aminosiloxane units. The ratio of organic groups to silicon atoms (R/Si) which was usually used to indicate the branched extent of a polysiloxane structure was 1.2. The synthesized reaction of the polysilicone was shown in Fig. 1.

Distilled water (25 ml), EtOH (75 ml) and TMAOH (1 ml) were mixed in a 250 ml flask under stirring. The mixture of PTMS, MTMS, DMDS and APS at certainly molar ratios (0.69: 0.06: 0.20: 0.05) was added to the above solution, maintaining 10% weight percentage. The stirring was stopped after 8 h, and the solution was aged at room temperature overnight. Precipitated condensate was collected by decantation of most clear supernatant, washed by vacuum filtration with distilled H_2O/EtOH (1/

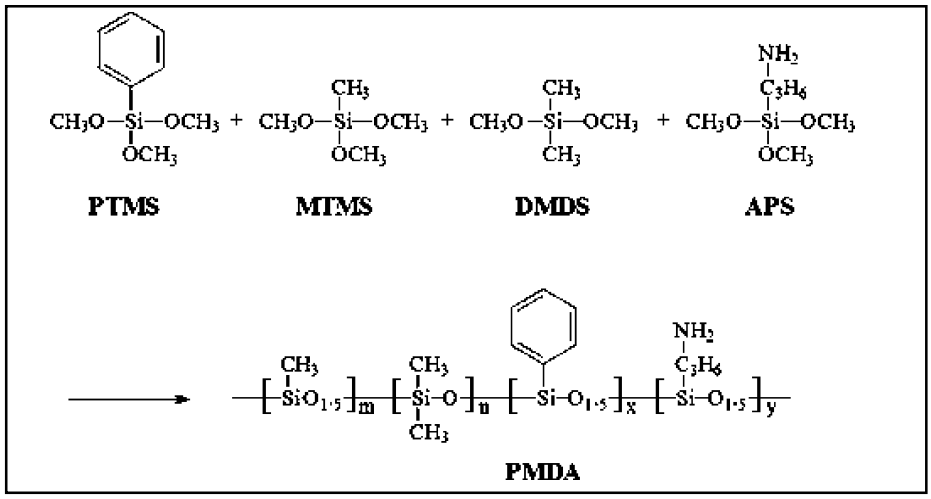

Fig. 1. Synthesis of PMDA

3 by volume), and then washed again in pure EtOH. The rinsed powder (PMDA) was dried thoroughly under vacuum for 20 h at room temperature.

2.3 Preparation of epoxy composites

Briefly, the EP/PMDA composites were prepared as follows: The PMDA was added into EPON 826 (75 g) and dispersed by a mechanical stirrer for 30 min. Subsequently, D230 (25 g) was added into the mixture and stirring for 30 min. And the content of PMDA was kept from 0 to 10 wt%. After degassed in vacuum for 10 min to remove any trapped air, the sample was cured at 80 °C for 2 h and post cured at 135 °C for 2 h.

2.4 Characterization and measurement

FTIR spectra of the dried samples were recorded using a Broker Equinox-55 IR spectrometer at a resolution of 2 cm^{-1} with 20 scans. The samples were mixed with potassium bromide and pressed to a disc, which was used to measure. Dynamic mechanical thermal analysis (DMA) was determined using a Rheometric Scientific SR-5000 dynamic mechanical analyzer. Data were collected from 40 °C to 140 °C at a scanning rate of 5 °C/min. Cone calorimeter measurement was performed on an FTT cone calorimeter (Britain) according to ASTM E1354 with heat flux of 50 kW/m^2. The dimensions of each specimen was 100×100×3 mm^3. The limiting oxygen index (LOI) was measured on an oxygen index instrument JF-3 produced by Jiangning Analysis Instrument Factory and performed according to GB2406-93. Thermogravimetric analysis (TGA) was carried on a TA instrument Q5000 thermogravimetric analyzer. The sample (about 10 mg) was heated from 50 °C to 600 °C at a set heating ramp rate in nitrogen atmosphere.

3. RESULTS AND DISCUSSION

3.1 Characterization of PMDA

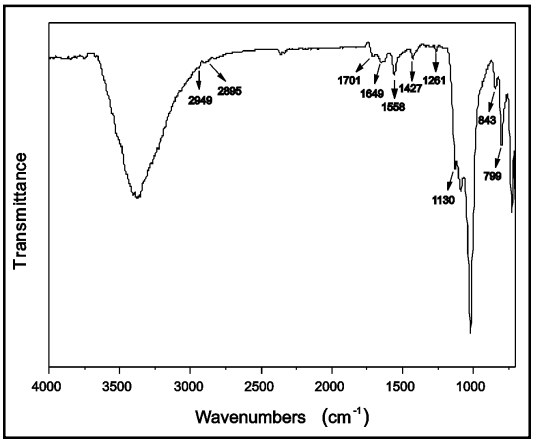

Fig. 2 FTIR spectra of PMDA

FTIR spectra of PMDA was shown in Fig. 2. The strong peak at 1200-1000 cm^{-1} characteristic of the Si-O-Si stretching vibration was clearly seen. The presence of Si-CH_3 was proven at 1261 cm^{-1} and an asymmetric stretching vibration of -CH_3 emerged at 2949, 2895 cm^{-1}. The curve exhibited a well-defined -C_3H_6-NH_2 group in PMDA at 2835 cm^{-1} (ν_{C-H}), 1649 cm^{-1} (ν_{N-H}), 1427 cm^{-1} (δ_{C-H}). The stretching vibrations of -C_6H_6 was observed at 1491 cm^{-1} ($\nu_{benzene\ ring}$). A broad peak around 3500 cm^{-1} could be attributed both to the adsorbed water and to the hydrogen-bonded Si-OH group. The above results indicated that PMDA has been successfully synthesized.

3.2 Methanical properties

Fig. 3 presented the storage modulus and tan delta of pure EP and EP/5 wt% PMDA (FREP) composites as a function of temperature. As shown in Fig. 3(a), the storage modulus curve of FREP composite was almostly in coincidence with pure EP. Moreover, the glass transition temperature (Tg) was widely determined by the tan delta peak temperature in DMA. As shown in Fig. 3(b), there was a slight reduction in Tg (ca. 0.1°C) at 5 wt% of PMDA than that of pure EP, indicating the movements of polymer chain wasn't restricted by the incorporation of PMDA.

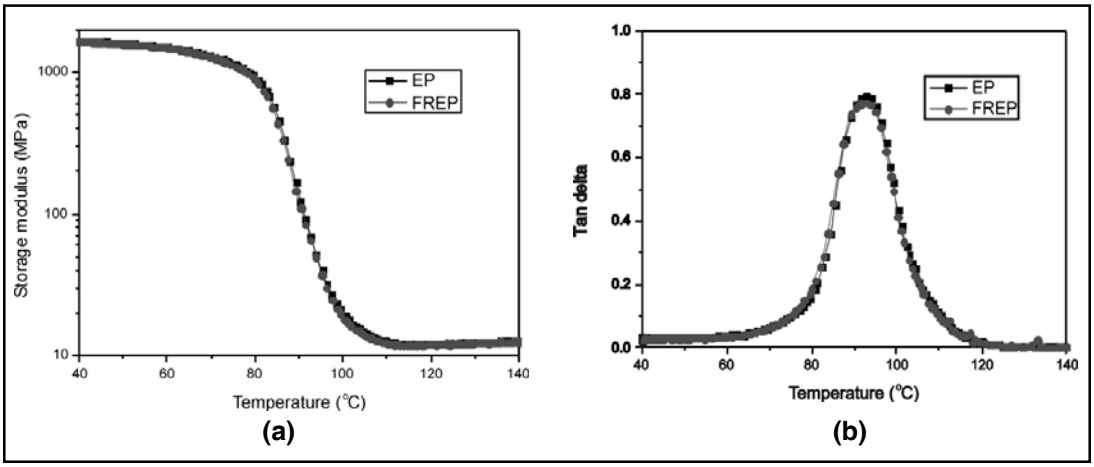

Fig. 3. Storage modulus (a) and tan delta (b) curves foar EP and FREP in the DMA test

3.3 Flame retardancy

The flame retardancy of EP/PMDA composites was investigated by the LOI, as shown in Fig. 4. It could be observed that the LOI value of pure EP was only 19.2%. With the incorporation of 9 wt% PMDA, the LOI value of EP was leveled up to 26.6%. It was reported that the Si-O unit could form a silicon-containing layer to retard the flame formation [17-18].

Cone calorimetry are widely used to evaluate the combustion performance of various materials under realworld fire conditions. The EP composites was exposed to a constant heat flux, while heat release rate (HRR, a measure

of a material's flammability) and total heat release (THR) were measured. Fig. 5 presented the HRR and THR vs. time curves of EP and its composites. The pure EP was highly flammable, exhibiting a peak heat release rate (PHRR) as high as 1737 kW/m^2. Compared to pure EP, FREP exhibited a lower PHRR, a 23.1% decrease than that of pure EP, indicating the higher fire safety consisting of 5 wt% PMDA. Fig. 5b revealed that the THR values of EP composites showed a similar trend to that of the PHRR. FREP exhibited a lower THR value than pure EP. At a 5 wt% loading of PMDA, the THR of FREP was reduced to 125.1 MJ/m^2, a 16.8% reduction compared with pure EP.

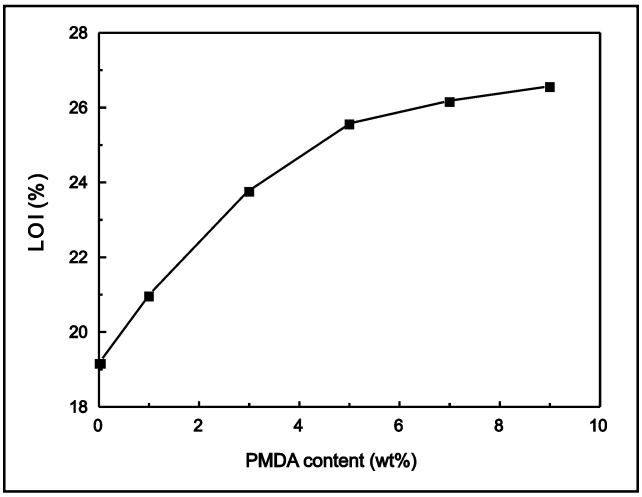

Fig. 4. The LOI of EP/PMDA composites

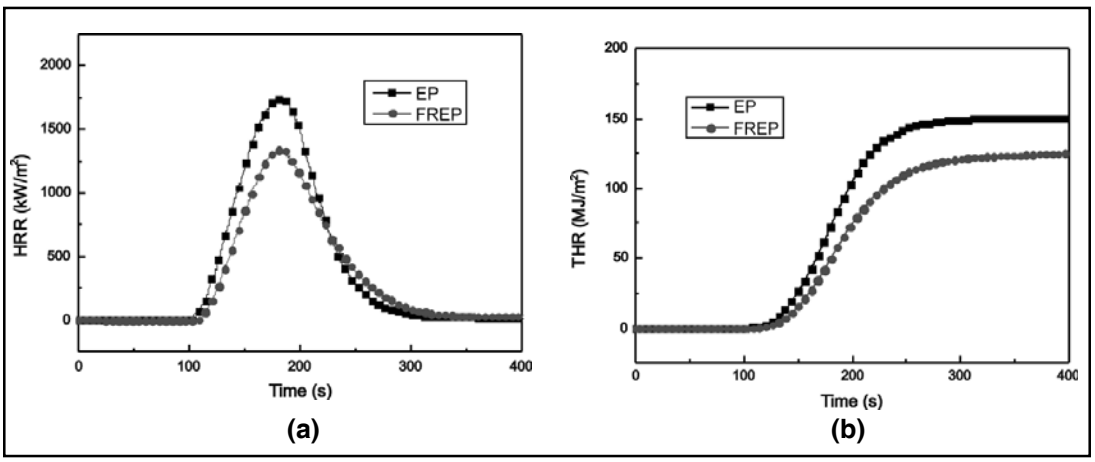

Fig. 5. HRR(a) and THR(b) curves of EP composites

3.4 Thermal stability

The TGA and DTG curves for EP and FREP composites observed in nitrogen atmosphere with a heating rate of 10°C/min were given in Fig. 6, and the characteristic weight loss data were listed in Table 1. It could be seen that EP and FREP composites both exhibited one step degradation process and rarely no weight loss up to 300°C.

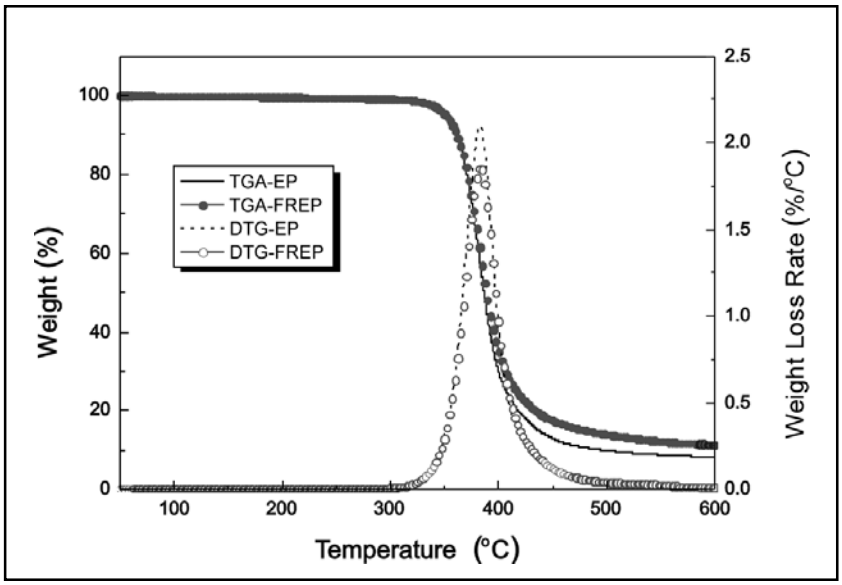

Fig. 6 Thermal stability of EP composites

TABLE 1. TGA data of EP composites

	Temperature (°C)		Peak rate (wt%/°C)	Residual char (wt%)
	$T_{5wt\%}$	T_{max}		
EP	351.7	382.6	2.10	8.27
FREP	350.8	383.1	1.86	11.34

The onset degradation temperature ($T_{5wt\%}$, 350.8°C) of FREP was slightly lower than the value 351.7°C of pure EP, which was mainly caused by the condensation of residual silanols groups of PMDA. However, the temperature of weight loss peak rate (T_{max}) was enhanced by the addition of PMDA. The peak rates of EP and FREP were corresponding to 2.10 wt%/°C and 1.86wt%/°C, emerged at 382.6°C and 383.1°C, respectively. Furthermore, in a comparison of the residues char amounts of EP with FREP, there was 3.13 wt% more

residues of the latter than of the former at 600°C. This result suggested that the PMDA could induce crosslinking reactions of EP during the thermal degradation process, and promoted the formation of the residual char which might play an important role for the increase of flame retardancy for EP composite.

3.5 Thermal degradation kinetics

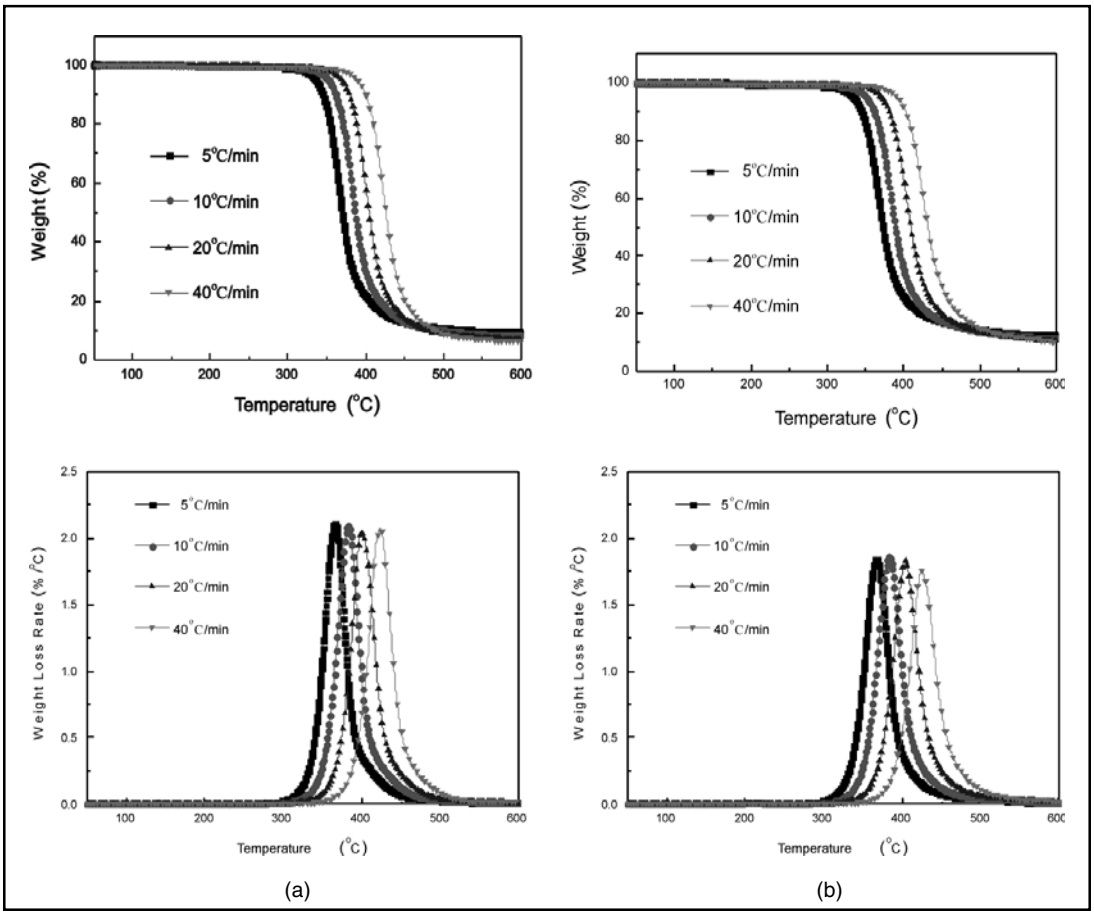

Fig. 7. TGA and DTG curves of EP (a) and FREP (b) composites

The TGA and DTG curves of EP and FREP at different heating rates in nitrogen atmosphere were shown in Fig. 7. All curves exhibited only single weight loss stage in the temperature range of 300-500°C. With increasing the heating rate from 5 to 40°C/min, the degradation curves of pure EP shifted to higher temperatures and then the onset degradation temperature enhanced. The same trend was observed for FREP composite.

Kinetic parameters of thermal degradation can be used to characterize the thermal stability of polymer and the activation energy (E) can be considered as a semiquantitative factor. According to the TGA and DTG curves in Fig. 7, the thermal degradation processes of EP and FREP can be studied by the Kissinger and Flynn-Wall-Ozawa methods, respectively.

1) Kissinger method [19]

The Kissinger expression is as follows:

$$\ln(\frac{\beta}{T_{\max}^2}) = \ln(\frac{AR}{E}) - \frac{E}{RT_{\max}} \qquad (1)$$

Where, β is the heating rate, T_{max} is the temperature of the peak rate, A is the absorbance, R is a gas constant, E is the activation energy for the thermal degradation process.

Firstly, according to the equation (1), the plots of In (β / T_{max}^2) versus $1/T_{max}$ were drawn and shown in Fig. 8, which indicated that there was a good linear relationship between In (β / T_{max}^2) and $1/T_{max}$. Then, the thermal degradation activation energies for EP and FREP could be obtained from the slope of corresponding straight line, and the pre-exponential factors were calculated from intercepts of the straight lines for samples. The calculation results for EP and FREP composites predicted by the Kissinger method were shown in Table 2.

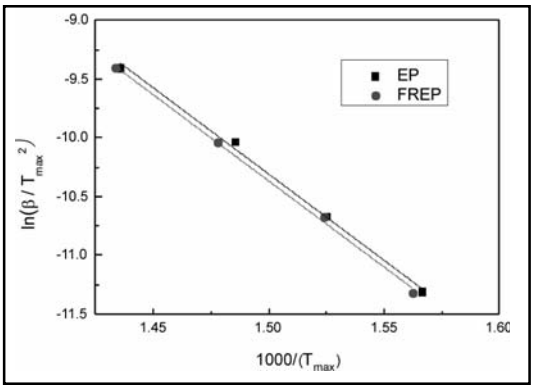

Fig. 8. The curves of In $(\frac{\beta}{T_{max}^2})$ vs. $\frac{1}{T_{max}}$ of EP and FREP

TABLE 2. Kinetic data for degradation of EP and FREP by Kissinger method

	T_{max} (°C)				E(kJ/mol)	lnA(1/min)
	5°C/min	10°C/min	20°C/min	40°C/min		
EP	365.4	382.6	400.1	423.5	122.1	14.4
FREP	367.0	383.1	403.4	424.6	121.9	14.3

It could be found that the activation energy for the thermal degradation process of FREP (121.9kJ/mol) was slightly lower than that of pure EP (122.1kJ/mol). It revealed that the flame retardant PMDA was effective to decrease the thermal degradation activation energy and promoted the thermal degradation process of EP.

2) Flynn-Wall-Ozawa method [20-21]

Because of the relative limitation of the Kissinger method, its data can only provide information at the peak temperatures. To make this possible, the TGA data is further studied by Flynn-Wall-Ozawa kinetic analysis method. Flynn-Wall-Ozawa method is one of the integral

methods that can determine the activation energy without knowledge of reaction order and differential data of TGA. With the application of that method, more informative kinetic parameters are obtained.

The equation of Flynn-Wall-Ozawa method can be expressed as follows:

$$\lg(\beta) = \lg AE / g(a)R - 2.315 - 0.457\frac{E}{RT} \quad (2)$$

Where, a is the degree of conversion, g (a) is the integrated forms of mechanism.

The above equation shows that lg(β) is linearly proportional to 1/T. The activation energy for any particular degree of degradation can then be determined by a calculation of the slope from the lg(β) – 1/T plots.

Based on the datum of Fig. 7 and the equation of $a = \frac{w_0 - w_t}{w_0 - w_\infty}$ (w_0 the initial weight of the sample, w_t the sample weight at any temperature t, w_∞ the final sample weight), the degree of conversion as a function of temperature relative to the degradation of both EP and FREP could be obtained, as shown in Fig. 9.

According to equation (2), the plots of lg(β) versus 1/T could be obtained and the typical lg(β) versus 1/T plots from 0.02 to 0.98

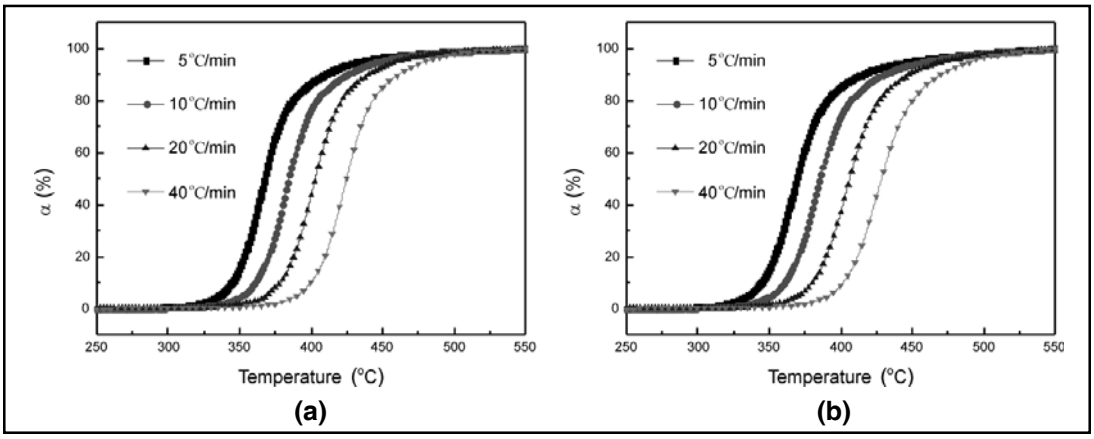

Fig. 9 Conversion of EP (a) and FREP (b) in function of temperature

conversion for the degradation of EP and FREP were shown in Fig. 10. It was clear that lg(β) was linearly proportional to 1/T. The activation energy for any particular degree of conversion could then be determined by a calculation of the slope from the plots. The activation energies of degradation calculated from these plots by Flynn-Wall-Ozawa method were shown in Fig. 11.

It was clearly shown that the activation energy curves of EP and FREP were quite similar and both increased with the increase of conversion degree in the whole thermal degradation process. Specifically, in the early and middle period of degradation, the activation energies of EP and FREP both increased slightly as degradation process, and then remain constant up to 90%, indicating that the stabilities of the

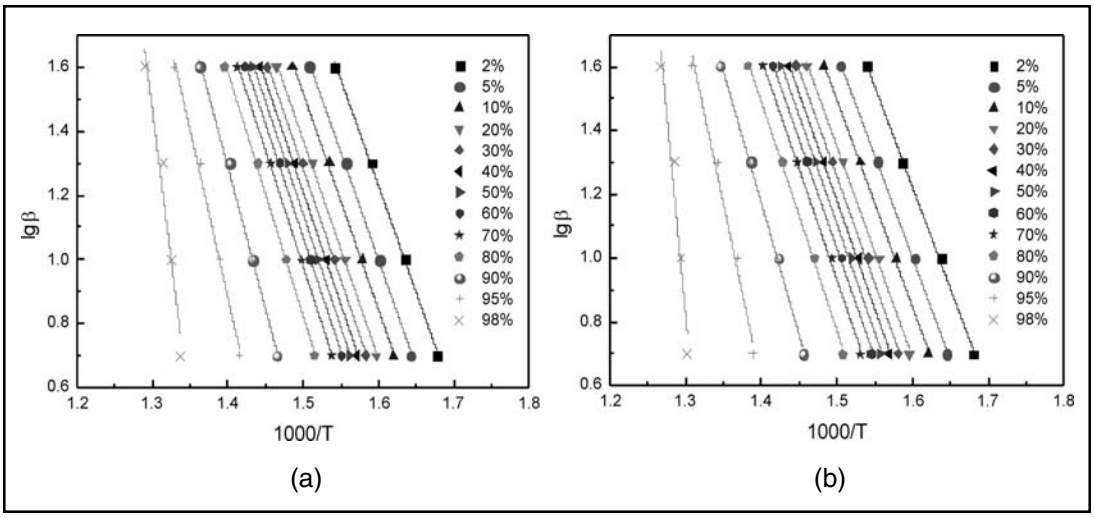

Fig. 10. The curves of lg*(β)* vs. 1/T of EP (a) and FREP (b)

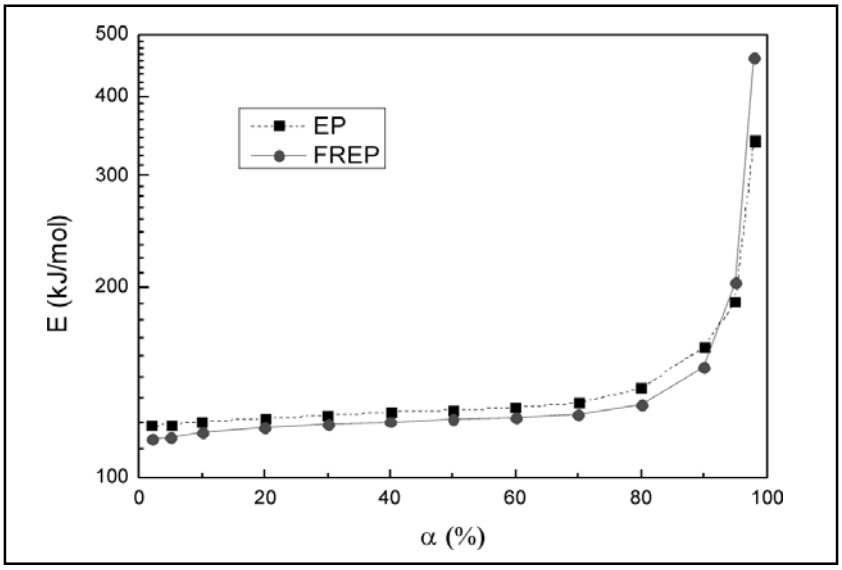

Fig. 11. Activation energy curves of EP and FREP by Flynn-Wall-Ozawa method

intermediate products were rather similar. Moreover, when the conversion degree of thermal degradation was less than 90%, the activation energy of FREP was lower than that of pure EP. In the final stage ($\alpha \geq 90\%$), the activation energies for EP and FREP progressively increased with increasing the conversion degree, indicating that the thermal

degradation mechanism varies with the weight loss. Comparing with the activation energies of EP and FREP, it could be obtained that the addition of PMDA further increased the EP activation energy in the final stage of thermal degradation, revealing that the PMDA had the function of stabilizing the char residue in the final period of thermal degradation process and finally improved the flame retardancy of EP.

4. CONCLUSION

In this study, a novel silicon-containing flame retardant PMDA was synthesized and added into epoxy resin (EP). EP/PMDA (FREP) exhibited lower peak heat release rate (PHRR) and total heat release (THR) by cone calorimeter measurement, in which 23.1% and 16.8% reduction were achieved compared with those of pure EP, respectively. Furthermore, the thermal degradation behavior of EP composites was investigated by the TGA measurement under non-isothermal conditions. Kissinger and Flynn-Wall-Ozawa methods were successfully employed to analyze the thermal degradation process. The results showed that PMDA remarkable enhanced the activation energy of EP thermal degradation in the final stage, which illustrated that the PMDA stabilized the char residues and improved the flame retardancy of EP in the final period of thermal degradation process.

Acknowledgement

The authors wish to thank the Ningbo Natural Science Foundation (2017A610067).

REFERENCES

1. H. Gu, C. Ma, J. Gu, J. Guo, X. Yan, J. Huang, Q. Zhang and Z. Guo. *J. Mater. Chem. C,* 2016, 4, 5890-5906.
2. H. Huang, K. Zhang, J. Jiang, J. Li and Y. Liu. *Polym. Int.,* 2017, 66, 85-91.
3. X. Zhao, H.V. Babu, J. Llorca and D.Y. Wang. *RSC Adv.,* 2016, 6, 59226-59236.
4. L. Chen, S.G. Chai, K. Liu, N.Y. Ning, J. Gao, Q.F. Liu, F. Chen and Q. Fu, *Acs Appl. Mater. Inter.,* 2012, 4(8), 4398-4404.
5. E.D. Weil and S. Levchik. *J. Fire Sci.,* 2004, 22(1), 25-40.
6. S. Liu, H. Yan, Z.P. Fang and H. Wang. *Compos. Sci. Technol.,* 2014, 90, 40-47.
7. R. Jian, P. Wang, W. Duan, J. Wang, X. Zheng and J. Weng. *Ind. Eng. Chem. Res.,* 2016, 55, 11520-11527.
8. A.B. Morgan and C.A. Wilkie. Flame retardant polymer nanocomposites. John Wiley & Sons, 2007.
9. A. Covaci, S. Harrad, M.A.E. Abdallah, N. Ali, R.J. Law, D. Herzke and C.A. de Wit. *Environ. Int.,* 2011, 37, 532-556.
10. C.A. de Wit, D. Herzke and K. Vorkamp. *Sci. Total Environ.,* 2010, 15, 2885-2888.
11. J.B. Wang, Y.Y. Zhan, J.H. Fang and H.Q. Gao. *J. Appl. Polym. Sci.*, 2012, 123(2), 1024-1031.
12. K. Wu, L. Song, Y. Hu, H. Lu, B.K. Kandola and E. Kandare. *Prog. Org. Coat.,* 2009, 65(4), 490-497.
13. W.J. Wang, L.H. Peng and G.H. Hsiue. *Polymer,* 2000, 41, 6113-6120.
14. G.H. Hsiue, W.J. Wang and F.C. Chang. *J. Appl. Polym. Sci.,* 1999, 73, 1231-1238.
15. Q. Wu, C. Zhang, R. Liang and B. Wang. *J. Therm. Anal. Calorim.,* 2010, 100, 1009-1015.
16. L.A. Mercado, M. Galia, J.A. Reina. *Polym. Degrad. Stab.,* 2006, 91, 2588-2594.
17. S.T. Lin and S.K. Huang. *J. Polym. Sci., A: Polym. Chem.,* 1996, 34(10), 1907-1922.

18. S. Ahmad, A.P. Gupta, E. Sharmin, M. Alam and S.K. Pandey. *Prog. Org. Coat.,* 2005, 54(3), 248-255.

19. H.E. Kissinger. *Anal. Chem.,* 1957, 29(11), 1702-1706.

20. J.H. Flynn. *J. Polym. Sci. Pol. Lett.,* 1966, 4(5), 323-328.

21. J.H. Flynn. *J. Polym. Sci. Pol. Lett.,* 1967, 5(2), 191-196.

Received: 16-01-2018

Accepted: 16-03-2018